Free Energy Calculations and Molecular Dynamics Simulations of Wild-Type and Variants of the DNA-*Eco*RI Complex

Srikanta Sen and Lennart Nilsson
Center for Structural Biochemistry, Karolinska Institute, Department of Biosciences, Huddinge, Sweden

ABSTRACT Molecular dynamics simulations and free energy calculations of the wild-type *Eco*RI-DNA complex and several variants have been performed in aqueous solvent. In general, he theoretical estimations of the free energy differences ($\Delta\Delta A$) qualitatively agree well with the corresponding experimental data. The modifications which were experimentally found unfavorable compared to the wild-type complex were also found to be so in theoretical estimates. The mutant where the amino group of the base Ade^6 was replaced by a hydrogen atom eliminating one H-bond between the DNA and the protein, was experimentally found to be more stable than the wild-type complex. It was speculated that the modification also caused a structural relaxation in the DNA making $\Delta\Delta A$ favorable. Our theoretical estimate yields a positive $\Delta\Delta A$ in this case, but the difference is small, and no significant local structural relaxation was observed. The major H-bonds between the DNA and the protein in the wild-type complex are found to be maintained in the different mutants although the specific and non-specific interaction energies between the interacting the DNA bases and the protein residues are different in different mutants. The interaction pattern of the other nearby nucleotides are significantly influenced by each modification. Thus, the alteration of the non-specific interactions may also play an indirect role in determining the specificity of the complex. The interaction of the Gua^4 of the DNA with the protein is found to be most sensitive to any alteration in the recognition site. Because Gua^4 is the nucleotide closest to the scissile bond, this extra sensitivity seems to play an important role in altering the functional activity of the complex.

INTRODUCTION

*Eco*RI is experimentally the most studied restriction endonuclease and is now used as one of the prototypes in understanding the physical basis of biomolecular recognition (Draper, 1993; Kim et al., 1990; Newman et al., 1994; Lesser et al., 1990; Robinson and Sligar, 1993, 1994; Venclovas et al., 1994; Misra et al., 1994). *Eco*RI binds to DNA specifically to the base sequence $d(GAATTC)_2$ and, in the presence of Mg^{+2} ion as a cofactor, it cuts both the DNA strands by hydrolyzing the sugar-phosphate backbone at the position between G and A in the recognition base sequence. In the companion paper we report the results of a detailed study of the structural, interactional and dynamical aspects of the wild-type DNA-*Eco*RI complex in aqueous solution by molecular dynamics (MD) simulation (Sen and Nilsson, 1999). However, like the other restriction endonucleases, *Eco*RI shows extreme selectivity in its interaction with DNA. Alteration in a single basepair in the recognition site can affect its binding affinity and functional activity substantially (Lesser et al., 1990, 1993). To characterize the different specific interactions considerable experimental work has been done, and plenty of experimental data on the free energy differences measured in biochemical experiments is available for different mutations made in the recognition site base sequence of the DNA in the DNA-*Eco*RI complex (Lesser et al., 1990, 1993). Experimental data show that a mutation resulting from a chemical modification of a functional group of a base in the recognition site is associated with a free energy difference of 1 to 2 kcal/mol, whereas an entire basepair substitution causes a larger free energy difference of about 10 kcal/mol (Lesser et al., 1990, 1993). On the other hand, theoretical estimation of the free energy differences in biomolecular interactions by molecular simulations (MD or Monte Carlo) is quite common nowadays (Bash et al., 1987; Cieplak et al., 1990; Härd and Nilsson, 1993; Elofsson et al., 1993; Miyamoto and Kollman, 1993; Eriksson and Nilsson, 1995; Essex et al., 1997; Soares et al., 1998). In the present work, we have performed such calculations by MD simulations for several cases of the mutant variants of the DNA-*Eco*RI complex. Because calculating the free energy differences due to mutations in biomolecular systems is very time consuming, we have selected only a few specific cases for our study where mutation has been made in a DNA base in the recognition site by altering a functional group that is known to be involved in direct interaction with the protein in the wild-type complex. The objective of the present work is twofold. One aspect is to calculate the free energy differences in the cases of the selected mutants by chemical perturbation and molecular dynamic simulation methods and to compare these values with the corresponding experimental data in order to see how successfully the modeling studies can describe the intermolecular interactions and the stability difference between the wild-type DNA-*Eco*RI complex and its different mutant variants. The other aspect is to characterize the structural and interactional properties of each of the mutant variants of the complex considered, comparing

Received for publication 4 December 1998 and in final form 13 July 1999.
Address reprint requests to Lennart Nilsson, Center for Structural Biochemistry, Karolinska Institute, Department of Biosciences, Halsovagen 7, Floor 7, S-141 57 Huddinge, Sweden. Tel.: 46-8-608-9228; Fax: 46-8-608-9290; E-mail: lennart.nilsson@csb.ki.se.

0006-3495/99/10/1801/10 $2.00

those to the corresponding wild-type complexes to identify the differences introduced in the properties of the complex due to the individual mutations in each case. For this purpose we have performed additional ordinary MD simulations of each of these mutants. It is particularly interesting to point out that there are experimental data for cases where the same chemical modification made on the same base at two different positions has resulted in opposite effects on the stability of the complex (Lesser et al., 1993). Mutation by replacing the NH_2 group at the atomic position 6 of the first adenine base in the recognition site by a hydrogen atom is experimentally found to be unfavorable by a free energy difference of 1.3 ± 0.2 kcal/mol, which is consistent with the fact that a H-bond with the protein is deleted by this mutation (Lesser et al., 1993; Draper, 1993). On the other hand, the same modification at the next adenine base of the DNA is experimentally found to be energetically favorable, as it is accompanied by a net negative free energy change of -1.0 ± 0.1 kcal/mol (Lesser et al., 1993), even though one H-bond with the protein is deleted in this case, too. In order to account for this observed preference for the change, it has been suggested that the resulting negative free energy difference in this case may be the consequence of the overall structural relaxation of the kink deformation of the DNA associated with this mutant complex (Lesser et al., 1993). In these experiments with different modified bases, it was further assumed that these individual modifications remove only the contribution of the particular functional group of the base which is modified and keep the other interactions between the base and the protein intact. So one of our major objectives in this study was to perform the free energy calculation and ordinary MD simulations of the fully solvated system in this second case and to compare the results with those for the wild-type complex, to obtain better insight into the details of what happens in these two cases and, if possible, to verify the above speculation and assumptions made in this case. It may also be noted that in the free energy calculations for each mutant, we have performed several independent dynamic simulations with different initial velocity conditions to avoid any initial condition-dependent bias in the estimated free energy differences. The estimated values of the free energy differences in the different cases of the mutants (except one case) show good qualitative agreement with the corresponding experimental results. However, the free energy estimates for such complex biomolecular systems by molecular simulations are generally associated with large statistical fluctuations resulting mainly from inadequate sampling of the conformational space. For the analysis and comparison of the structural and interactional aspects of the different mutants, we have looked into different average quantities from the dynamic trajectories and have compared them for all the mutant cases and the wild-type complex. We have also compared the interaction strengths and H-bond lists for all the mutants in order to have further details about the difference in the interaction patterns of the different mutants. The analysis of the local structure and interaction pattern in the mutation locality from ordinary MD simulations indicates that even a small specific alteration in the DNA-protein interaction can affect both the specific (DNA base and protein) and nonspecific (DNA backbone and protein) interactions of the other nearby nucleotides and the altered nonspecific interaction thus can have some role in determining the overall specificity of binding. On the whole, we feel that the results presented here, along with the corresponding experimental data, provide us with much more detailed insight into the DNA-protein interaction at the atomic level in the cases of different mutants of the DNA-*Eco*RI complex.

METHODS

Theory of free energy simulation

As the free energy calculation by chemical perturbation method is now a widely used technique, we will present only an outline of the basic theory (Fleischman and Brooks, 1987; King 1993; van Gunsteren et al., 1993; Straatsma et al., 1993). In thermodynamic perturbation method, one starts with a hybrid molecular system consisting of both the reactant and the product parts along with the environmental part. The Hamiltonian is constructed as follows, depending on the molecular coordinates (r) and a coupling parameter λ, as

$$H(\mathbf{r}, \lambda) = H_0(\mathbf{r}) + (1-\lambda)H_A(\mathbf{r}) + \lambda H_B(\mathbf{r}) \qquad (1)$$

which is modeled as the sum of $H_0(r)$ and a linear combination of $H_A(r)$ and $H_B(r)$, where $H_0(r)$ is the Hamiltonian of the system excluding the reactant and the product parts described by $H_A(r)$ and $H_B(r)$ respectively, evaluated at a given value of the coupling parameter λ through which the transformation takes place. λ can take values in the range of 0 to 1 where $\lambda = 0$ represents the perturbed part in the reactant state and $\lambda = 1$ corresponds to the product state of the same. In the thermodynamic perturbation method the free energy difference between two chemical states, A and B, is calculated by using the relation

$$\begin{aligned} \Delta A_{A \rightarrow B} &= \sum [A(\lambda_i) - A(\lambda_i + \Delta\lambda)] \\ &= -RT \sum \ln\langle \exp[\beta \Delta H(\lambda_i)] \rangle_{\lambda_i} \end{aligned} \qquad (2)$$

$$\Delta H(\lambda_i) = H(\lambda_i) - H(\lambda_i + \Delta\lambda) \qquad (3)$$

is the difference in the Hamiltonian between the two neighboring states defined by the coupling parameters λ_i and $\lambda_i + \Delta\lambda$, A is Helmholtz's free energy, H the Hamiltonian, $\beta = (RT)^{-1}$, R the gas constant, and T the absolute temperature. The symbol $\langle \cdots\cdots \rangle_{\lambda_i}$ denotes a time average of the quantity along the perturbation pathway characterized by the coupling parameter λ_i. Here the total perturbation is split into a number of smaller ones (between the coupling parameter values λ_i and $\lambda_i + \Delta\lambda$), called windows, for which accurate evaluation of the free energy differences by perturbation method may be possible. The total free energy difference between the two states is then obtained as the sum of the contributions from the individual windows (Eq. 2). Thus, performing sufficiently long MD simulations at different intermediate states of the hybrid system, one gets the time average of the quantity $\exp[\beta \Delta H(\lambda_i)]$ for each λ_i. By using them, one can estimate the free energy difference between two states of a system with the help of Eq. 2. Such calculations of free energy differences as mentioned above can subsequently be used for estimating the difference ($\Delta\Delta A$) of free energy differences (e.g., between ΔA_1 and ΔA_2) characterizing the stability difference in a biomolecular system (for example, a DNA-protein complex like the present case) due to a mutation from different transformation steps in a thermodynamic cycle, as explained

below. Consider the following thermodynamics cycle,

$$\begin{array}{ccc} & \Delta A_1 & \\ \text{DNA} + \text{Protein} & \rightarrow & \text{DNA-Protein} \\ \downarrow \Delta A' & & \downarrow \Delta A'' \\ \text{DNA}' + \text{Protein} & \rightarrow & \text{DNA}'\text{-Protein} \\ & \Delta A_2 & \end{array}$$

where DNA′ is the DNA with the mutation. Because the free energy is a thermodynamic state function, its value depends only on the end points and is independent of the actual path of transformation. Thus, in the above thermodynamic cycle one gets $\Delta\Delta A = \Delta A_1 - \Delta A_2 = \Delta A' - \Delta A''$; i.e., $\Delta\Delta A = \Delta A_1 - \Delta A_2$ can also be expressed equivalently as the difference $\Delta A' - \Delta A''$, which is easy to obtain from molecular simulations.

Description of the different chemical modifications

We have performed calculations for several cases of mutations on the DNA bases of the recognition part in the complex for which we have experimental data. In each of these mutants a functional group or atom of a relevant base has been replaced by another group or atom such that the formation of a crucial hydrogen bond between the DNA and the protein in the complex is eliminated. The different modifications used are described below.

A → ^{7}A: In this modified base the N7 atom of an adenine base is replaced by a CH group (Fig. 1 *a*)

G → ^{7}G: This represents the replacement of the N7 atom of a guanine base by a CH group (Fig. 1 *b*).

A → P: This is a modified adenine base where the NH_2 group at the position 6 is replaced by a hydrogen atom (Fig. 1 *c*).

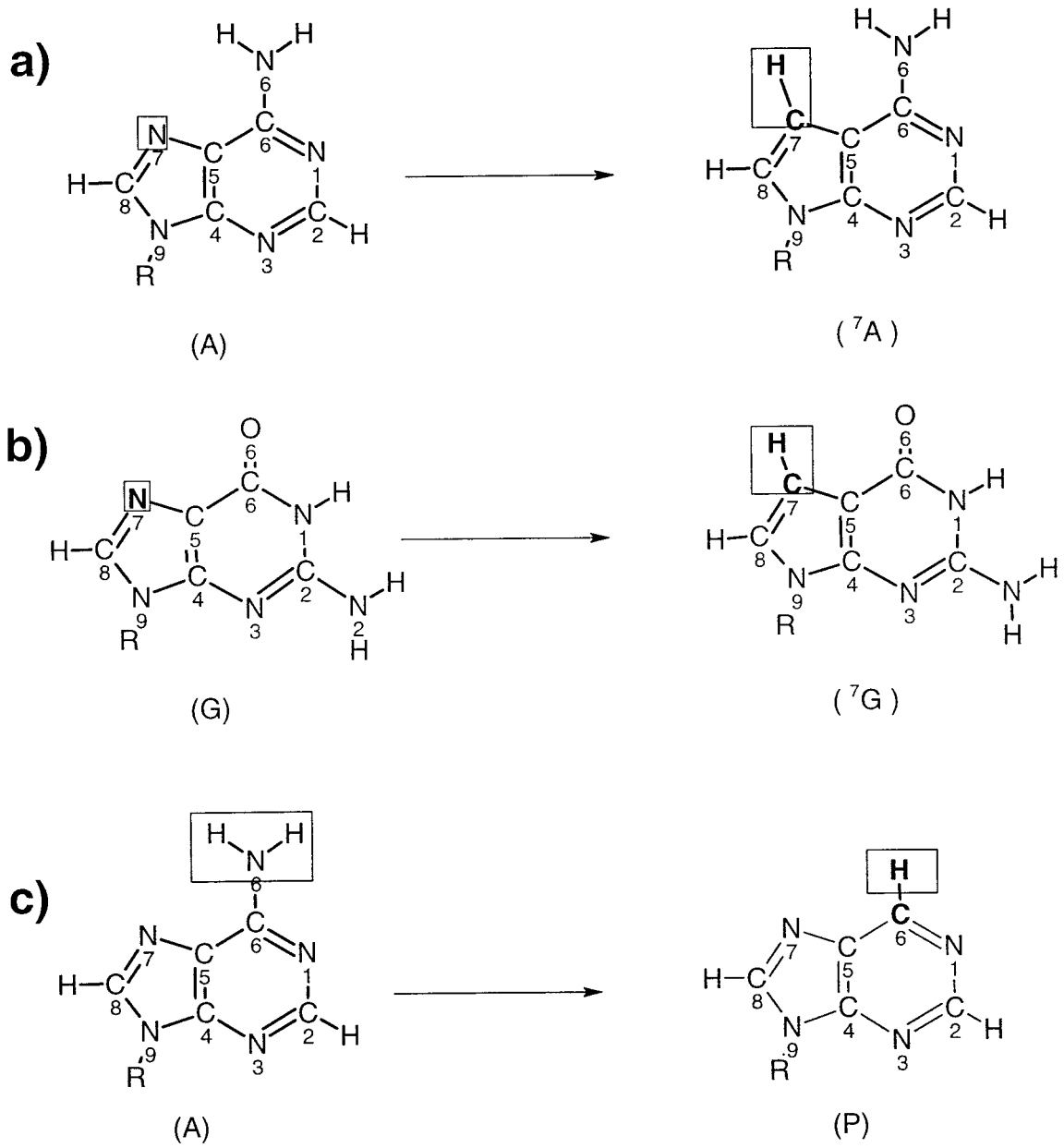

FIGURE 1 Schematic diagrams of the different modifications used in the present study. (*a*) The N7 atom of Adenine base is replaced by a C-H group. (*b*) The N7 atom of Guanine base is replaced by a C-H group. (*c*) The NH2 group of Adenine base is replaced by a hydrogen atom.

Charges

Because in these mutations the bases are partially modified, one needs to know the partial atomic charges of the modified base. Calculation of accurate partial atomic charges for a molecular system is a very difficult task and there is no unique, straightforward way of finding them on a rigorous level. In the present work we have adapted the following procedure. In each case, the partial atomic charges of the altered base in the product state were calculated by MOPAC 6.0 package using the AM1 parameter set and the electrostatic potential (ESP) fitting method (Steward, 1990). The atoms nearest to the product atoms in each case were considered the colocated atoms, whose charges were different in the reactant and product states. As a working approximation, we have used the calculated partial atomic charges for the product atoms and distributed the difference in the total charge of the product and colocated atoms between their calculated charges and the corresponding charges in CHARMM topology equally on the calculated charges of the colocated atoms to keep the net charge the same. The charges thus obtained for the product and colocated atoms in the different mutant bases are summarized in Table 1. The partial atomic charges of the other atoms in the base were kept as usual CHARMM charges to maintain an overall consistency with the other parameter set of CHARMM.

System setup for free energy perturbation

We have considered the following cases of mutants with a chemical modification and assigned a name (given in parentheses) to each case: (i) A → P is made at the base position 5 of the first strand (M1); (ii) A → P is made at the base position 6 of the first strand (M2); (iii) G → ^{7}G P is made at the base position 4 of the first strand (M3); (iv) A → ^{7}A is made at the base position 5 of the first strand (M4); and (v) A → ^{7}A is made at the base position 6 of the first strand (M5).

In order to calculate the free energy difference ΔΔA for each mutant we prepared two independent system setups, one for the DNA-protein complex in solution and the other for the free DNA in solution. In the case of the complex, starting from the energy-minimized crystallographic coordinates of the *Eco*RI-DNA complex, we cut out a part that was within a sphere of 16 Å radius with the nitrogen atom (N6 or N7, depending on the case) of the reactant part of the respective base in the mutation site at the center. The respective base in the mutation site was replaced by a hybrid system consisting of the normal base for the reactant state and the modified base for the product state in each mutant case. This system containing the hybrid part was then immersed in a pre-equilibrated TIP3P water sphere of 19 Å radius with the NH_2 group of the hybrid system at the center, and the water molecules whose oxygen atoms were within a distance of 2.8 Å from any non-hydrogen atom of the complex were removed (Jorgensen et al., 1983). To make the system electrically neutral we placed 13 Na^+ counterions by replacing 13 water molecules whose oxygen atoms had highest electrostatic energies and are >5 Å apart from each other. The system was then energy-minimized by 500 steepest descent steps, keeping the reactant and the product atoms of the hybrid part fixed. The energy-minimized system was then used for the MD simulation for free energy perturbation calculations. In all the energy minimization and subsequent dynamic simulations, the free ends of the backbone of the disjointed fragments of the protein created as a result of cutting out a sphere (16 Å radius) from the complex as mentioned above were kept harmonically constrained with a force constant of 10 kcal/mol/A^2 to preserve the effect of the natural covalent continuity of the protein backbone.

For the free DNA simulation, in a similar way, from the DNA in standard B-form corresponding to the DNA in the complex and containing the same hybrid part as in the complex, a sphere of 16.0 Å radius as mentioned above was cut out. Seventeen Na^+ counterions were included for electro-neutrality of the system and each counterion was placed at a distance 3.5 Å from the phosphorus atom on the line bisecting the line joining the two oxygen atoms of the respective phosphate group of this DNA fragment. The whole system was then solvated in a TIP3P water sphere of 19 Å radius and energy-minimized by 500 steepest descent steps, keeping the reactant and the product atoms of the hybrid part fixed, and was subsequently used in the MD simulation.

TABLE 1 Summary of partial atomic charges for the perturbed parts in different modified bases

Modification type	Atom name	Atom nature	Charge in reactant state	Charge in product state
A → ^{7}A	N7	reactant	−0.63	−
	C7	product	−	−0.26
	H7	product	−	0.25
	C5	colocated	0.23	−0.08
	C8	colocated	0.38	0.07
G → ^{7}G	N7	reactant	−0.69	−
	C7	product	−	−0.20
	H7	product	−	0.26
	C5	colocated	−0.08	−0.20
	C8	colocated	0.41	−0.22
A → P	N6	reactant	−0.80	−
	H61	reactant	0.40	−
	H62	reactant	0.40	−
	H7	product	0.22	0.22
	C6	colocated	0.43	0.35
	C5	colocated	0.23	0.16
	N1	colocated	−0.74	−0.81

System setup for stochastic deformable boundary (SDB) dynamics of mutants

To investigate the local structural and interactional characteristics of each of the different mutant variants at the modification site, we prepared the solvated complex in a way similar to that described above, except that in these cases we replaced the hybrid base with the modified base. Each such system was then subjected to SDB dynamics simulations.

Solvent shell setup for mutant M2

As the mutant M2 experimentally yields free energy value qualitatively quite different from those for other mutants, we treated the case of this mutant in more detail. For a direct comparison with the properties of the wild-type complex, we prepared the setup with the full complex M2 containing the modified part and fully solvated by a solvent shell 7 Å thick as described in the companion paper (Sen and Nilsson, 1999). Ordinary MD simulation was then performed on this system to investigate the details of the interactional and structural aspects of the particular case.

MD simulation protocol for the free energy difference calculations

In all the cases of mutants we have performed MD simulation of the solvated DNA-*Eco*RI complex system by SDB dynamics algorithm for sampling at different intermediate states using the standard CHARMM potential energy function and parameter set (Brooks et al., 1983; MacKerell et al., 1995, 1998) and the free energy perturbation implementation (Fleischman and Brooks, 1987). The atoms in the spherical shell (the buffer region) between radii 17 Å and 19 Å executed dynamics according to Langevin dynamics algorithm, whereas the atoms inside the sphere of 17 Å radius were subjected to ordinary MD, following leap-frog algorithm. The solvent molecules were subjected to a deformable boundary force arising from the mean field interaction of water molecules beyond the 19 Å boundary (Brooks and Karplus, 1983).

In the cases of free energy calculation for the mutants, the simulations were performed with a time step of 2 fs. We used 13.0 Å as the cutoff value for the nonbonded interactions and the nonbonded interaction list was

updated every 10 steps. We used force shift option causing the interaction energies and the forces to vanish smoothly at a distance of 12.0 Å. We also used the SHAKE algorithm (Ryckaert et al., 1977) for constraining all bonds involving hydrogen atoms. We used a dielectric constant of value 1.0. The system was connected to a heat bath at a temperature of 300K. All the non-hydrogen atoms were assigned a friction coefficient of 50 ps^{-1}. The system was first equilibrated at 300K with $\lambda = 0.5$ for 50 ps and then simulated in seven consecutive windows at seven λ values of 0.05, 0.125, 0.25, 0.50, 0.75, 0.875, and 0.95, respectively. In each window a 20-ps equilibration followed by a 40-ps production run was performed. We have kept the bond term and the bond angle term in the potential energy function unperturbed to maintain the structure of the perturbed part of the system for λ values close to the limiting values 0 or 1. We also used a double-wide sampling method over the full range of λ to calculate the overall free energy difference in the transformation. Simulation was performed in an identical way for the free DNA.

For each mutant, the same protocol for the dynamics equilibration and the production runs was followed. We performed at least three independent simulations on each of these systems, starting with a different initial velocity assignment, to get an idea of the initial velocity-dependent fluctuation in the computed values.

SDB dynamics of mutants

In the cases of setups with the modified bases in the product state to investigate the local structural and dynamical properties, SDB dynamics was performed following the same protocol as described above, without the perturbation part.

Solvent shell simulation of the mutant M2

In the case of the mutant M2, for direct comparison with the properties of the wild-type complex we have performed the ordinary molecular dynamics simulations of the fully solvated mutant complex M2 by a solvent shell 7 Å thick in the manner described in the companion paper (Sen and Nilsson, 1999).

TABLE 2 Summary of the estimated values of $\Delta A''$ and $\Delta A'$ in the different independent simulations for each of the cases of mutant variants considered

	$\Delta A''$ (kcal/mole)	$\Delta A'$ (kcal/mole)	$\Delta\Delta A = \Delta A'' - \Delta A'$ (kcal/mole)	Expt value (kcal/mole)
A: Modification A → P in the Ade^5 base in strand 1				
1	27.0	23.2	+3.8	
2	27.1	24.3	+2.8	
3	23.6	23.5	+0.1	
4	25.9	23.4	+2.5	
5	25.1	23.8	+1.3	
Aver	25.7 ± 1.3	23.6 ± 0.4	2.1 ± 1.2	+1.3 ± 0.2
B: Modification A → P in the Ade^6 base in strand 1				
1	25.4	22.8	+2.69	
2	25.5	23.8	+1.64	
3	22.8	24.5	−1.71	
4	24.8	22.2	+2.56	
5	24.1	23.5	+0.63	
Aver	24.5 ± 1.0	23.4 ± 0.8	1.1 ± 1.6	−1.0 ± 0.1
C: Modification G → ^{7}G in the Gua^4 base in strand 1				
1	−2.7	−7.2	+4.5	
2	−6.5	−7.9	+1.4	
3	−2.7	−7.6	+4.5	
Aver	−3.9 ± 1.8	−7.6 ± 0.3	3.5 ± 1.5	+1.4 ± 0.2
D: Modification A → ^{7}A in the Ade^5 base in strand 1				
1	−30.7	−30.5	−0.3	
2	−30.8	−29.9	−0.9	
3	−29.3	−30.4	+0.9	
Aver	−30.3 ± 0.7	30.3 ± 0.3	0.1 ± 0.7	+1.3 ± 0.2
E: Modification A → ^{7}A in the Ade^6 base in strand 1				
1	−21.3	−31.1	+9.7	
2	−24.4	−31.1	+6.7	
3	−25.7	−29.5	+3.8	
Aver	−23.8 ± 1.9	−30.6 ± 0.8	6.7 ± 2.4	+1.4 ± 0.2

$\Delta A''$ represents the free energy difference between the wild type and mutant variant in the complex while $\Delta A'$ corresponds to the case of the free DNAin each case.

RESULTS AND DISCUSSION

Free energy difference calculations

Table 2 summarizes the results of free energy calculations. It is seen that in all the mutations considered, the calculated free energy difference $\Delta\Delta A$ from MD simulations indicates that the chemical modifications make the resulting DNA-protein complex less favorable compared to the wild-type complex. This is consistent with the fact that in each case, a H-bond between the DNA and the protein is deleted. The computational data in most of the cases (except the case of M2) are thus in good qualitative agreement with the corresponding experimental data, although the quantitative agreements are not that good (Lesser et al., 1993). The calculated data also show considerable fluctuations in $\Delta\Delta A$ values obtained from different independent free energy perturbation simulations for the same mutant and it is noticeable that the root mean square fluctuation in the estimated free energy differences ($\Delta A'$) in the case of the complex are, in general, larger than the corresponding ΔA in the free DNA case. However, such statistical fluctuations are generally associated with the free energy calculations of complex macromolecular systems from molecular simulations. Several things seem to be responsible for these observed differences between the calculated average values of the free energy differences, the corresponding experimental data, and the significant fluctuations of the values obtained in different independent simulations. First, the empirical force field and the parameters used to describe such complex molecular systems may not be sufficiently accurate. Second, errors may be introduced due to finite sampling, which may not be adequate in all the cases studied. Finally, in such calculations, because $\Delta\Delta A$ (which is usually a small quantity) is estimated as the difference of two relatively large quantities, $\Delta A'$ and $\Delta A''$, significant errors are generally associated with it. Calculations show that, in general, a large change in free energy ($\Delta A'$ or $\Delta A''$) is associated with such chemical transformations. This large change in free energy actually arises due to the difference in the interaction energies of the perturbed base with the rest of the system in the native and modified cases. Thus, as it basically represents the difference in the average enthalpies of the native and the modified DNA, its actual value is not important for our present purpose and when a difference is taken to obtain $\Delta\Delta A$, this factor cancels out, as it is present in both the free DNA and the DNA in the complex.

The plot of the ΔA-vs.-λ curve for each mutant as represented in Figs. 2 and 3 demonstrate how the cumulative value of ΔA varies with λ in the free DNA (*dashed line*) and in the complex (*solid line*) for the different mutants. It may be noted that even in cases of the same chemical modification but at different base positions, there are some differences in the nature of the plots. The reason seems to be the difference in the microscopic nature of the neighborhood. However, these are not physically very relevant, as the states of the hybrid system in the range $0 < \lambda < 1$ represents unphysical chemical states of the system and, the free energy being a thermodynamic state function, only the end point values are important.

Comparison of root mean square deviations (RMSD)

Because the DNA in the complex contains a distorted kinked part at the center of the recognition sequence and the modifications are made in the bases in the locality of the kink, the DNA is the most likely molecular component where significant structural relaxation may occur. We have compared the average RMSD of the central five bases (GAATT) of the DNA recognition site (to avoid the end effects) containing the kink for all the different mutants. The results are presented in the Table 3. Comparison shows very similar RMSD values for this part in all the different mutant cases, indicating that there is no exceptional structural relaxation of the kink of the DNA in any of these cases, including the mutant M2, where a significant relaxation was postulated. However, in reference to the wild-type complex the average values of the RMSD in the individual cases of the mutants are found to be larger, as expected.

Fig. 4 compares the average RMSD of the individual nucleotides of the DNA. It is found that generally, for the different mutants, larger structural rearrangements occurred than in the wild-type complex, and the effects of these small modifications extend over a substantial part of the DNA.

Comparison of interaction pattern

Comparison of the specific (DNA base and protein) and nonspecific (DNA backbone and protein) interaction ener-

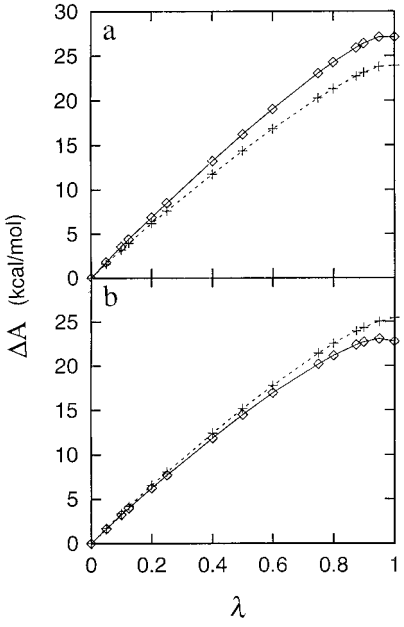

FIGURE 2 The variation of the accumulated free energy difference (DA) in the different cases of mutations. *Solid lines* represent the case of the complex and the *dashed line* corresponds to the free DNA simulation in the cases of mutants M1 (*a*) and M2 (*b*).

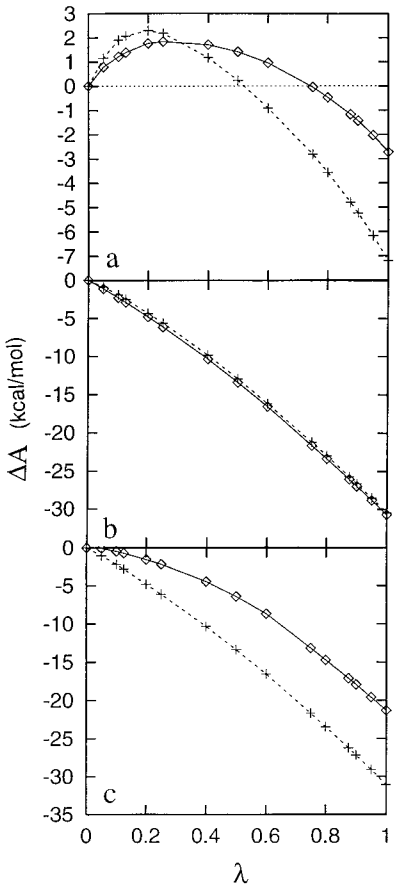

FIGURE 3 The variation of the accumulated free energy difference (DA) in the different cases of mutations. *Solid lines* represent the case of the complex and the *dashed line* corresponds to the free DNA simulation in the cases of mutants M3 (*a*), M4 (*b*), and M5 (*c*).

TABLE 3 Comparison of RMSDs

System	Average RMSD (Å)
M1	2.0 ± 0.1
M2	1.4 ± 0.1
M3	1.7 ± 0.1
M4	1.4 ± 0.1
M5	1.5 ± 0.1
Wild-type	1.1 ± 0.1

Comparison of the average RMSD of the region (GAATT) of the recognition sequence of the DNA strand DNA1 containing the kink for the different mutant variants and the wild-type complex.

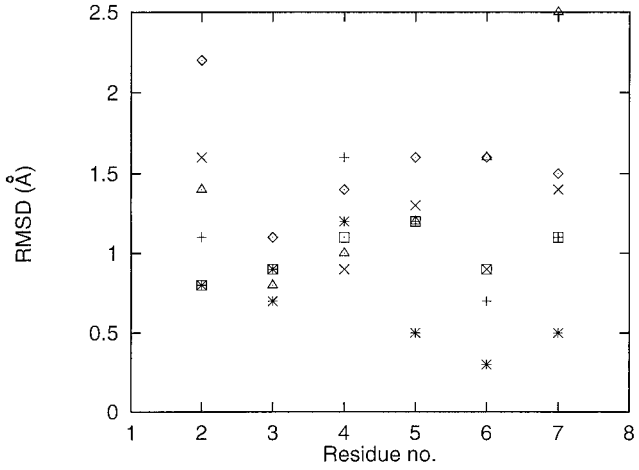

FIGURE 4 Comparison of the average RMSD of the individual bases of the recognition site of the DNA strand DNA1 against the nucleotide number. The symbols ◇, +, □, ×, △, and ✳ represent the cases of the mutant variants M1, M2, M3, M4, M5, and the wild-type complexes, respectively.

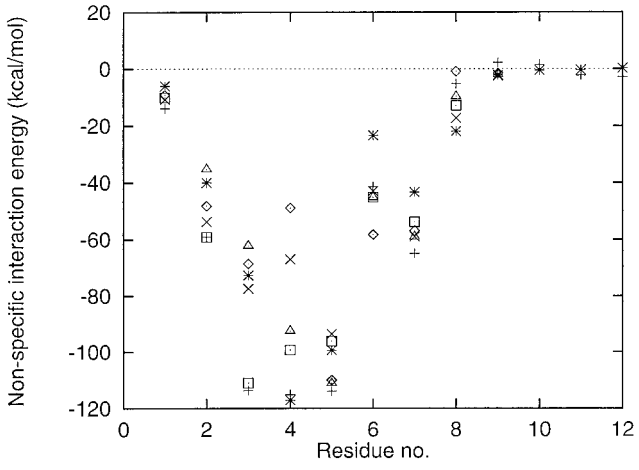

FIGURE 6 Comparison of the average nonspecific interaction energies of the individual bases of the DNA strand DNA1 with the entire protein against the nucleotide number. The symbols ◇, +, □, ×, △, and ✳ represent the cases of the mutant variants M1, M2, M3, M4, M5, and the wild-type complexes, respectively.

gies in the average structures of the different mutant variants and the wild-type of the complex in aqueous solvent indicates that even these small changes in a specific functional group or atom of a single base can induce significant changes both in the specific (Fig. 5) and nonspecific (Fig. 6) interaction pattern of the individual bases, and the influence is extended over at least a few basepairs around the modification sites. The quantity $\Delta E = E_{mutant} - E_{wt}$ can be used as a measure of the specificity of a particular modification, where E_{mutant} and E_{wt} represent the total energy of interaction between the DNA and the protein in the mutant and the wild-type complex, respectively. If ΔE is large it means that the modification strongly affects the specificity, whereas an ΔE value ~ 0 indicates a nonspecific nature of the modification. Again, ΔE can be expressed as $\Delta E = \Delta E$ (specific) $+ \Delta E$ (nonspecific), where ΔE (specific) comes from the difference in the direct specific interaction and ΔE (nonspecific) represents the difference resulting from the altered nonspecific interaction part. This clearly indicates that even a difference in nonspecific interaction due to a modification can significantly contribute to the overall specificity of the modification site.

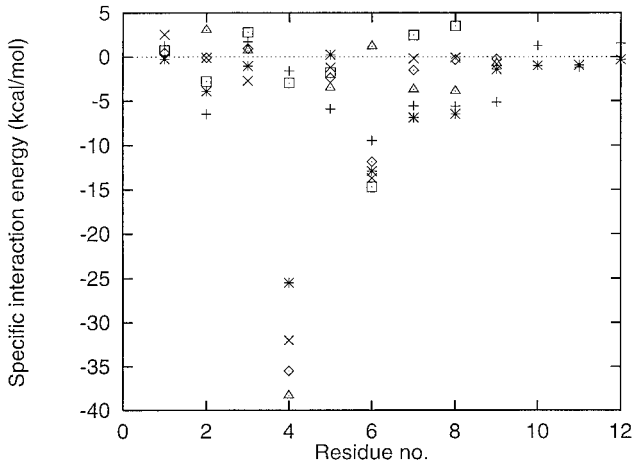

FIGURE 5 Comparison of the average specific interaction energies of the individual bases of the DNA strand DNA1 with the entire protein, against the nucleotide number. The cases of the mutant variants M1, M2, M3, M4, M5, and the wild-type complexes are represented by the symbols ◇, +, □, ×, △, and ✳ respectively.

It was also found that both specific and nonspecific interactions of the Gua^4 and the protein are highly sensitive to the modifications made at other bases in the recognition site. It is, then, quite interesting to identify Gua^4 as the first base in the recognition site on the DNA strand and one of the two bases closest to the scissile bond where the DNA strand is cut by the protein. It may also be noticed that in some of the mutants, the interaction energies between some DNA nucleotides and the protein are strikingly similar, though for others they are quite different (Figs. 5 and 6). However, in all the cases except that of the $Ade^5 \rightarrow P$ modification, the interaction strengths at the modified base are changed maximally. It was also found that these modifications not only affected the interactions of the bases of the modified DNA strand with the protein, but also influenced the interactions of the other DNA strand and the protein as well, though to a lesser extent. Thus, even the effects of small modifications are found to be quite complicated as the whole complex behaves as a single integrated system.

Table 4 summarizes the comparison of the specific, nonspecific, and overall intermolecular interaction energies between the GAATT part of the recognition sequence on the first strand (DNA1) of the DNA duplex and the protein. It can be seen clearly that each of these quantities is quite different for the different mutants and the wild-type complex. However, the overall relative stability of a complex is

TABLE 4 Interaction energies

Mutant	Specific (kcal/mol)	Nonspecific (kcal/mol)	Total intermolecular interaction energy (kcal/mol)
M1	−49.7	−242.1	−291.8
M2	−25.9	−313.9	−339.8
M3	−4.9	−407.8	−412.7
M4	−47.1	−239.9	−287.0
M5	−48.6	−277.9	−326.5
Wild-type	−51.5	−305.1	−356.6

Comparison of the interaction energy of the sequence part (GAATT) of the DNA1 strand from the average structure of the mutants and wild type complexes.

governed by the total free energy difference between the two states of the DNA and the protein where they are free in solution and in bound form as a complex in solution, and thus these values cannot be directly correlated with the relative stabilities of these mutant variants. These results are presented mainly to demonstrate that such small modifications may also cause significant differences in the overall intermolecular interactions between the DNA and the protein.

Protein-DNA H-bonds

Comparison of the H-bond list (Table 5, A and B) between the DNA (in the modification site) and the protein for all the mutant variants and the wild-type complex clearly indicates that most of the major H-bonds between the modified base and the protein seen in the wild-type complex are also well maintained in the solution-simulated structures of the different mutant variants. This is also true for the other neighboring bases which preserve their H-bonding with the protein. However, the interaction energies are changed significantly in all these different mutants (Figs. 5 and 6). The alteration in the interaction energy strengths in each case is caused by altered interaction geometry of the interacting atoms as a result of small local rearrangements due to the chemical modifications. It may be noted in Table 2 that in the case of the mutant M4, the theoretically estimated values of ΔΔA are small in all the independent calculations and, in the H-bond lists, it is found that the H-bond involving N7 atom of Ade^{6} is not strong. Thus, these results are consistent with each other.

The special case of the mutant M2

The case of this mutant variant is of special interest, as it was mentioned earlier that the experimental value of ΔΔA for this mutant (M2) is negative (−1.0 kcal/mol), indicating that the mutated complex is more stable than the wild-type complex. It was then speculated (Lesser et al., 1993) that this mutant variant must be associated with a structural relaxation of the kink in the DNA, resulting in an overall favorable change in free energy. However, the theoretically computed value of ΔΔA from MD simulation in this case gives an average value of 1.1 ± 1.6 kcal/mol (Table 2), indicating that the mutation in this case is also less stable than the wild-type complex. This result contrasts qualitatively with the experimental data (Table 2), even though the difference (2.1 kcal/mol) from the experimental value is similar to the other cases, and it is consistent with the fact that this mutant also lacks a functional group on the DNA base that interacts with the protein through a H-bond in the wild-type complex. The calculated positive values of ΔΔA in most of the independent simulations with this mutant clearly indicate the generality of this result. For better

TABLE 5A Major H-bonds in mutant variants

Residue or nucleotide	Mutation M1		Mutation M2		Wild-type	
	H-bond	Ave. lt (ps)	H-bond	Ave. lt (ps)	H-bond	Ave. lt (ps)
Gua^{4}	O1P–HZ2 Lys^{148} *Eco*RIa	10.8	O1P–HD21 Asn^{141} *Eco*RIb	25.9	O1P–HD22 Asn^{141} *Eco*RIb	6.6
	O2P–HN Lys^{89} *Eco*RIa	20.4	–HH12 Arg^{203} *Eco*RIb		–HH12 Arg^{203} *Eco*RIb	12.9
	O6–HH22 Arg^{200} *Eco*RIb	11.4	O2P–HN Lys^{89} *Eco*RIa	19.4	O2P–HZ2 Lys^{148} *Eco*RIa	74.2
	N7–HH12 Arg^{203} *Eco*RIb	47.0	–HZ3 Lys^{148} *Eco*RIa		N7–HH22 Arg^{200} *Eco*RIb	23.6
Ade^{5}	O1P–HH11 Arg^{145} *Eco*RIa	54.9	O1P–HZ3 Lys^{148} *Eco*RIa	33.1	O1P–HH22 Arg^{145} *Eco*RIa	297.0
	HH22 Asn^{149} *Eco*RIa		O2P–HZ1 Lys^{113} *Eco*RIa	118.5	O2P–HZ1 Lys^{113} *Eco*RIa	74.5
	O2P–HZ1 Lys^{113} *Eco*RIa	38.4	05′–HH11 Arg^{145} *Eco*RIa	12.9	05′–HH11 Arg^{145} *Eco*RIa	13.2
	05′–HH11 Arg^{145} *Eco*RIa	27.6	N7–HD22 Asn^{141} *Eco*RIb	6.2		
	N7–HD22 Asn^{141} *Eco*RIb	14.1	H61–OD1 Asn^{141} *Eco*RIb	23.6		
Ade^{6}	O1P–HN Hse^{114} *Eco*RIa	32.0	O1P–HN Hse^{114} *Eco*RIa	238.0	O1P–HN Hse^{114} *Eco*RIa	59.4
	N7–HH12 Arg^{145} *Eco*RIa	16.8	N7–HH12 Arg^{145} *Eco*RIa	52.9	N7–HH12 Arg^{145} *Eco*RIa	74.5
Thy^{7}	O1P–HN Gly^{116} *Eco*RIa	14.6	O1P–HN Gly^{116} *Eco*RIa	94.2	O1P–HN Gly^{116} *Eco*RIa	22.4
	O2P–HN Gly^{116} *Eco*RIa	20.0	O4 HN Asn^{141} *Eco*RIa	7.8		
	–HZ2 Lys^{117} *Eco*RIa					
	O4–HD22 Asn^{141} *Eco*RIa	13.2				
Thy^{8}	O1P–HZ3 Lys^{117} *Eco*RIa	52.0	O1P–HZ3 Lys^{117} *Eco*RIa	56.7	O2P–HZ2 Lys^{117} *Eco*RIa	20.3
	O4–HN Gly^{140} *Eco*RIa	8.5				

List of major H-bonds in the mutant variants M3, M4, and M5. The criterion used for identifying a H-bond is $D_{HA} \langle 2.5$ Å and $Angle_{D\text{-}H\text{-}A} \rangle 135$, where D_{HA} is the distance between the hydrogen and the acceptor and $Angle_{D\text{-}H\text{-}A}$ is the angle made by the donor-H-acceptor.
Ave. lt, average lifetime.

TABLE 5B Major H-bonds in M3, M4, and M5

Residue or nucleotide	Mutation M3		Mutation M4		Mutation M5	
	H-bond	Ave. lt (ps)	H-bond	Ave. lt (ps)	H-bond	Ave. lt (ps)
Gua[4]	O1P–HH12 Arg[203] *Eco*RIb	16.4	O1P–HZ1 Lys[148] *Eco*RIa	39.9	O1P–HZ3 Lys[148] *Eco*RIa	11.6
	–HH12 Arg[203] *Eco*RIb		O2P–HNLys[89] *Eco*RIa	8.8	O6–HH22 Arg[200] *Eco*RIb	26.2
	O2P–HZ3 Lys[148] *Eco*RIb	81.3	N7–HH12 Arg[203] *Eco*RIa	53.5	N7–HH12 Arg[203] *Eco*RIb	22.4
			–HH21 Arg[203] *Eco*RIa			
Ade[5]	O1P–HH11 Arg[145] *Eco*RIa	20.1	O1P–HH11 Arg[145] *Eco*RIa	42.9	O1P–HZ1 Lys[148] *Eco*RIa	131.6
	–HH11 Arg[145] *Eco*RIa		–HH22 Arg[145] *Eco*RIa		O2P–HH11 Arg[145] *Eco*RIa	118.4
	O2P–HZ1 Lys[113] *Eco*RIa	247.0	O2P–HZ1 Lys[113] *Eco*RIa	17.7	–HZ1 Lys[113] *Eco*RIa	
	O5′–HH11 Arg[145] *Eco*RIa	13.1	O5′–HH11 Arg[145] *Eco*RIa	17.4	O5′–HH11 Arg[145] *Eco*RIa	28.7
	N7–HD22 Asn[141] *Eco*RIb	6.0	H61–OD1 Asns[141] *Eco*RIb	338.8	N7–HD22 Asn[141] *Eco*RIb	16.8
	H61–OD1 Asns[141] *Eco*RIb	43.8			H61–OD1 Asns[141] *Eco*RIb	105.8
Ade[6]	O1P–HN Hse[114] *Eco*RIa	249.0	O1P–HZ3 Lys[113] *Eco*RIa	37.4	O1P–HN Hse[114] *Eco*RIa	67.5
	N7–HH12 Arg[145] *Eco*RIa	13.0	N7–HH12 Arg[145] *Eco*RIa	13.3		
Thy[7]	O1P–HZ2 Lys[117] *Eco*RIa	16.0	O1P–HN Gly[116] *Eco*RIa	14.0	O2P–HN Gly[116] *Eco*RIa	17.1
			O2P–HN Gly[116] *Eco*RIa	9.6		
Thy[8]	O1P–HZ3 Lys[117] *Eco*RIa	49.0	O1P–HZ3 Lys[117] *Eco*RIa	33.3	O1P–HZ2 Lys[117] *Eco*RIa	37.9

List of major H-bonds in the mutant variants M3, M4, and M5. The criterion used for identifying a H-bond is $D_{HA} \langle 2.5$ Å and $Angle_{D\text{-}H\text{-}A} \rangle 135$, where DHA is the distance between the hydrogen and the acceptor and $Angle_{D\text{-}H\text{-}A}$ is the angle made by the donor-H-acceptor.
Ave. lt, average lifetime.

insight into what actually happened in this case, we analyzed the 700-ps trajectory of the whole complex with this mutant. Comparison of the RMSD of the individual nucleotides of the DNA (Fig. 4) does not reveal any indication of any significant difference. The average torsion angles of the nucleotide Ade[6] (Table 6A) and of the side chain Asn[141] (Table 6B), which interacts with the Ade[6] base in the wild-type complex, also indicates very similar local structures in the wild-type complex and in the mutant variant.

It is possible that the wild-type conformation from which our simulations were started is kinetically stable enough for this mutant that a larger relaxation cannot be achieved in a finite simulation. Thus, we find that the result of the free energy calculation from our simulations in this case does not agree with the corresponding experimental data and in the present dynamic simulation we did not find any evidence of significant relaxation of the DNA kink as suggested by the experimental group. Our theoretical estimate of ΔΔA for this mutant obtained from several independent simulations is, however, completely consistent with the fact that we have not observed any structural relaxation in the DNA.

TABLE 6A Average torsional angles of Ade[6]

Tor. angle	Mutant M2	Wild-type
α	−111.7 ± 13.8	−105.6 ± 13.1
β	146.5 ± 13.4	133.9 ± 11.5
γ	49.8 ± 8.9	52.6 ± 8.8
δ	142.5 ± 6.7	143.2 ± 6.2
ε	−106.4 ± 16.0	−111.4 ± 19.1
ζ	146.4 ± 15.4	147.2 ± 16.3
χ	−111.4 ± 10.1	−107.3 ± 9.3

Comparison of the average torsional angles of the DNA nucleotide Ade[6] between the wild-type complex and the mutant variant M2.

SUMMARY AND CONCLUSION

MD simulations and free energy calculations of the wild-type *Eco*RI-DNA complex and several mutant variants have been performed in aqueous solvent to gain insight about the interaction and recognition mechanism of the complex. The main results we obtained are summarized here.

1. The calculated free energy differences by chemical perturbation and dynamic simulation methods are found to be in qualitative agreement with the corresponding experimental data in most of the cases of the mutants considered here except one, although the values are in general overestimated. In the case of the mutant M2 we obtained a positive value for the ΔΔA value in contrast to the experimental data, which shows a negative value.

2. Comparison of the average backbone torsional angles of Ade[6] of DNA1 and Asn[141] of *Eco*RIb between the mutant M2 and the wild-type complexes does not show any indication of local structural relaxation of the complex in the mutant M2. This shows that the experimental negative ΔΔA is not likely to be a result of local differences and thus suggests that something else, like a conformational change over larger part of the molecule, is indeed necessary.

3. Comparison of the interaction pattern and the intermolecular H-bonding pattern in the different mutant vari-

TABLE 6B Average torsional angles of Asn[141]

Tor. angle	Mutant M2	Wild-type
$\theta 1$	−73.8 ± 8.6	−71.4 ± 6.8
$\theta 2$	−5.6 ± 16.1	−18.7 ± 25.7
$\theta 3$	2.1 ± 13.9	−3.7 ± 17.2

Comparison of the average torsional angles of the *Eco*RIb residue Asn[141] between the wild type complex and the mutant variant M2. $\theta 1$, $\theta 2$, and $\theta 3$ are the torsion angles C-CA-CB-CG, CA-CB-CG-OD1 and CB-CG-ND2-HD21, respectively, of the residue Asn[141] of the protein monomer *Eco*RIb.

ants with reference to the wild-type complex indicates that the individual modifications in the bases eliminate the particular interactions involving the modified group but maintain the other major interactions of the base with the protein, as assumed in the experiments. However, both the specific and nonspecific interaction energies between the interacting pairs of the DNA nucleotides and the protein residue are different in the cases of different mutants and the interaction pattern of the other nearby nucleotides are significantly influenced by the modification. This implies that the alteration of the nonspecific interactions may also play some indirect role in determining the specificity of the complex.

4. The interaction pattern of the Gua^4 of the DNA with the protein was found to be most sensitive to any alteration on the bases in the recognition site. As Gua^4 is the nucleotide closest to the scissile bond, this extra sensitivity may play an important role in altering the functional efficiency of the complex.

We acknowledge the financial support of the Swedish Natural Science Research Council for the present work.

REFERENCES

Bash, P. A., U. C. Singh, F. K. Brown, R. Langridge, and P. A. Kollman. 1987. Calculation of the relative change in binding free energy of a protein-inhibitor complex. *Science* 235:574–576.

Brooks, B. R., R. E. Bruccoleri, B. D. Olafson, D. J. States, S. Swaminathan, and M. Karplus. 1983. CHARMM: a program for macromolecular energy minimization and dynamics calculations. *J. Com. Chem.* 4:187–217.

Brooks III, C. L., and M. Karplus. 1983. Deformable stochastic boundaries in molecular dynamics. *J. Chem. Phys.* 79:6312–6325.

Cieplak, P., S. N. Rao, P. D. J. Grootenhuis, and P. A. Kollman. 1990. Free energy calculations on base specificity of drug-DNA interactions: applications to daunomycin and acridin intercalation into DNA. *Biopolymers.* 29:717–727.

Draper, D. E. 1993. Protein-DNA complexes: the cost of recognition. *Proc. Natl. Acad. Sci. USA.* 90:7429–7430.

Elofsson, A. T. Kulinski, R. Rigler, and L. Nilsson. 1993. Site specific point mutations change specificity: a molecular modeling study by free energy simulations and enzyme kinetics of the thermodynamics in ribonuclease T1 substrate interactions. *Proteins Struct. Funct. Genet.* 17:161–175.

Eriksson, M., and L. Nilsson. 1995. Structure, thermodynamics and cooperativity of glucocorticoid receptor DNA-DNA-binding domain in complex with different response elements: molecular dynamics and free energy perturbation study. *J. Mol. Biol.* 253:453–472.

Essex, J. W., D. L. Severance, J. Tirado-Rives, and W. L. Jorgensen. 1997. Monte Carlo simulations for proteins: binding affinities for trypsin-benzamidine complexes via free energy perturbations. *J. Phys. Chem.* 101:9663–9669.

Fleischman, S. H., and C. L. Brooks III. 1987. Thermodynamics of aqueous solvation: solution properties of alcohols and alkanes. *J. Chem. Phys.* 87:3029–3037.

Härd, T., and L. Nilsson. 1992. Free energy calculations predict sequence specificity in DNA-drug complexes. *Nucleosides Nucleotides.* 11: 167–173.

Jorgensen, W. L., J. Chandrasekhar, J. D. Madura, R. W. Impey, and M. L. Klein. 1983. Comparison of simple potential functions for simulating liquid water. *J. Chem. Phys.* 79:926–935.

Kim, Y., J. C. Grable, R. Love, P. J. Green, and J. M. Rosenberg. 1990. Refinement of EcoRI endonuclease crystal structure: a revised protein chain tracing. *Science.* 249:1307–1309.

King, P. M. 1993. Free energy via molecular simulation: a primer. *In* Computer Simulations of Biomolecular Systems: Theoretical and Experimental Applications, Vol. 2. W. F. van Gunsteren, P. K. Weiner, and A. J. Wilkinson, eds. ESCOM, Leiden, The Netherlands. 267–314.

Lesser, D. R., M. R. Kurpiewski, T. Waters, B. A. Connolly, and L. Jen-Jacobson. 1993. Facilitated distortion of the DNA site enhances EcoRI endonuclease-DNA recognition. *Proc. Natl. Acad. Sci. USA.* 90:7548–7552.

Lesser, D. R., M. R. Kurpiewski, and L. Jen-Jacobson. 1990. The energetic basis of specificity in the EcoRI endonuclease-DNA interaction. *Science.* 250:776–785.

MacKerell, A. D., Jr., D. Bashford, M. Bellott, R. L. Dunbrack, Jr., J. D. Evanseck, M. J. Field, S. Fischer, J. Gao, H. Guo, S. Ha, D. Joseph-McCarthy, L. Kuchnir, K. Kuczera, F. T. K. Lau, C. Mattos, S. Michnick, T. Ngo, D. T. Nguyen, B. Prodhom, W. E. Reiher, III, B. Roux, M. Schlenkrich, J. C. Smith, R. Stote, J. Straub, M. Watanabe, J. Wiorkiewicz-Kuczera, D. Yin, and M. Karplus. 1998. All-atom empirical potential for molecular modeling and dynamics: studies of proteins. *J. Phys. Chem. B.* 102:3586–3616.

MacKerell, Jr., A., J. Wiorkiewicz-Kuczera, and M. Karplus. 1995. An all-atom empirical energy function for the simulation of nucleic acids. *J. Am. Chem. Soc.* 117:11946–11975.

Misra, V., J. L. Hecht, K. A. Sharp, R. A. Friedman, and B. Honig. 1994. Salt effects on protein-DNA interactions: the λcI repressor and EcoRI endonuclease. *J. Mol. Biol.* 238:264–280.

Miyamoto, S., and P. A. Kollman. 1993. Absolute and relative binding free energy calculations of the interaction of biotin and its analogues with streptavidin using molecular dynamics/free energy perturbation approaches. *Proteins Struct. Funct. Genet.* 16:226–2455.

Newman, M., T. Strzelecka, L. F. Dorner, I. Schildkraut, and A. K. Aggarwal. 1994. Structure of restriction endonuclease BamHI and its relationship to EcoRI. *Nature.* 368:660–664.

Robinson, C. R., and S. G. Sligar. 1993. Molecular recognition mediated by bound water: a mechanism for star activity of the restriction endonuclease EcoRI. *J. Mol. Biol.* 234:302–306.

Robinson, C. R., and S. G. Sligar. 1994. Hydrostatic pressure reverses osmotic pressure effects on the specificity of EcoRI-DNA interactions. *Biochemistry.* 33:3787–3793.

Ryckaert, J. P., G. Ciccotti, and H. J. C. Berendsen. 1977. Numerical integration of the Cartesian equations of motion of a system with constraints: molecular dynamics of n-alkanes. *J. Comp. Phys.* 23: 327–341.

Sen, S., and L. Nilsson. 1999. Structure, interaction, dynamics, and solvent effects on the DNA-EcoRI complex in aqueous solution from molecular dynamics simulation. *Biophys. J.* 77:1782–1800.

Soares, C. M., P. J. Martel, J. Mendes, and M. A. Carrondo. 1998. Molecular dynamics simulation of cytochrome c3: studying the reduction processes using free energy calculations. *Biophys. J.* 74:1708–1721.

Straatsma, T. P., M. Zacharias, and J. A. McCammon. 1993. Free energy difference calculations in biomolecular systems. *In* Computer Simulations of Biomolecular Systems: Theoretical and Experimental Applications, Vol. 2. W. F. van Gunsteren, P. K. Weiner, and A. J. Wilkinson, eds. ESCOM, Leiden, The Netherlands. 349–367.

Steward J. J. P. 1990. MOPAC: a semiempirical molecular orbital program. *J. Computer Aided Mol. Des.* 4:1–45.

van Gunsteren, W. F., T. C. Beutler, F. Fraternali, P. M. King, A. E. Mark, and P. E. Smith. 1993. Computation of free energy in practice: Choice of approximations and accuracy limiting factors. *In* Computer Simulations of Biomolecular Systems: Theoretical and Experimental Applications, Vol 2. W. F. van Gunsteren, P. K. Weiner, and A. J. Wilkinson, eds. ESCOM, Leiden, The Netherlands. 315–348.

Venclovas, C., A. Timinskas, and V. Syksnys. 1994. Five stranded β-sheet sandwiched with two α-helices: a structural link between restriction nucleases EcoRI and EcoRV. *Proteins Struct. Funct. Genet.* 20: 279–282.